Monatshefte für Chemie - Chemical Monthly
https://doi.org/10.1007/s00706-024-03227-y

ORIGINAL PAPER

Covalent modification of chitosan surfaces with a sugar amino acid and lysine analogues

Tobias Dorn[1] · Matjaž Finšgar[2] · Karin Stana Kleinschek[1] · Tobias Steindorfer[1] · Martin Thonhofer[1] · Tanja M. Wrodnigg[1] · Rupert Kargl[1,3]

Received: 19 December 2023 / Accepted: 12 June 2024

Abstract

This work explores the modification and characterization of chitosan thin films as a model for functionalized polysaccharide interfaces. The solid–liquid interface of oligo- and polysaccharides is crucial for various biological processes such as cell adhesion and recognition. By covalent surface modification of the chitosan via amide formation with different small molecules containing carboxylic acids, e.g. specially designed glycoside hydrolase inhibitors, interactions with biomolecules and living cells could potentially be controlled in the future. As a first step towards this aim, three fluorescent compounds were conjugated onto nanometric chitosan thin films. The layers were analysed by fluorescence spectroscopy, X-ray photoelectron spectroscopy, time-of-flight secondary ion mass spectrometry, and atomic force microscopy, to proof the covalent attachment of the target molecules. By this analysis, a uniform and chemically stable covalent attachment of the target molecules on the chitosan thin films could be demonstrated under various conditions. This publication serves as a proof-of-concept-study for further biofunctionalization, pattering, and interaction studies involving polysaccharide interfaces, glycosidase inhibitors, proteins, or living cells.

Graphical abstract

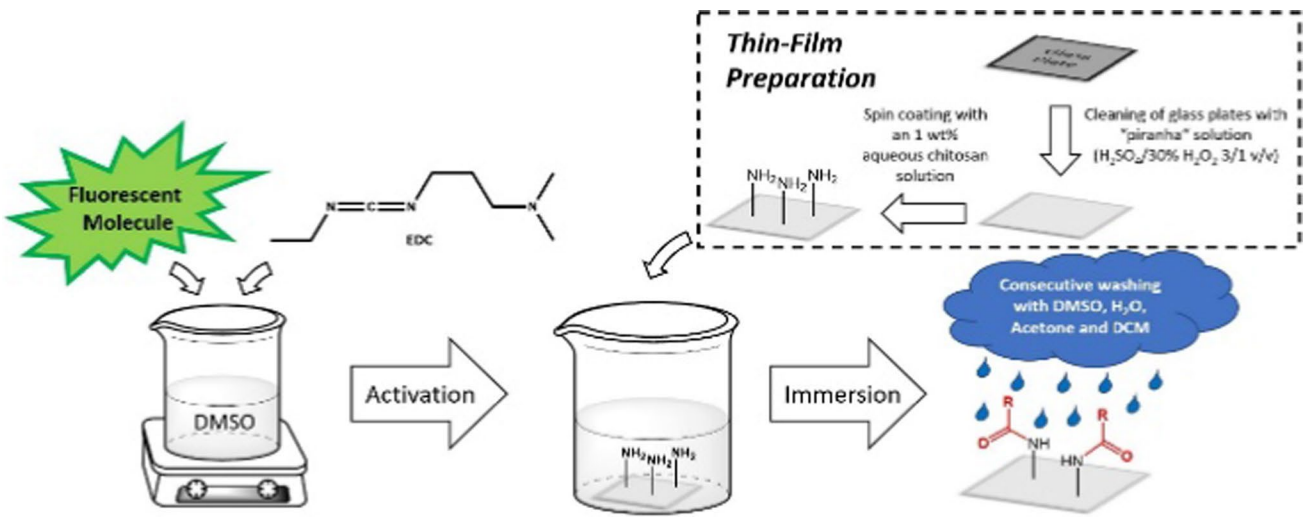

Keywords Carbohydrates · Fluorescence spectroscopy · Amino acids · Chitosan · Thin film modification · *C*-Glycosides

Extended author information available on the last page of the article

Published online: 03 August 2024

Introduction

The solid–liquid interface of oligo- and polysaccharides is of importance in biology and medicine, for cell adhesion and recognition. Examples of such interfaces include the peptidoglycan layers in bacteria [1], the chitin layers in fungi [2], and many other cell-wall and extracellular poly- and oligosaccharides [3]. Chitin in fungal cell walls for instance is covered by other glycans and by mannosylated proteins [2]. Knowledge about the preparation of well-defined semi-synthetic polysaccharide interfaces can therefore be very relevant for basic interaction studies such as protein (lectin) binding [4], antibody–antigen interaction [5], or enzymatic degradation [6]. It has been shown that iminosugar-based glycosidase inhibitors can be immobilized on synthetic polyamine bearing surfaces, to specifically capture and inhibit these enzymes [7]. The present work extends this concept to the immobilization of similar molecules to the polyamine and polysaccharide chitosan, and investigates in detail the conditions and analysis necessary for covalent chemical surface modification.

Polyamine surfaces can be prepared by chemical synthesis [8], adsorption through dip coating [9], or spin coating [10]. A subsequent attachment of molecules to these layers can contribute to further bio-functionalization and can alter and control the interaction with biomolecules [11] or living cells [12]. In the long term, this could lead to new applications for diagnostics [13], as biomaterial coatings [14], or for (bio-)separation [15].

An interesting molecule for surface bio-functionalization in this respect is 6-aminohexanoic acid (AHX) or aminocaproic acid, a lysine analogue, approved procoagulative drug [16], and polyamide monomer [17]. Due to its abundance and biological relevance, and due to its similarity to the lysine residues of proteins, it can be an interesting spacer and an anchor for further attachments or modifications of surface layers.

Another class of compounds of biological interest is so called amino-sugar acids (ASA), which have a carbohydrate, a carboxyl, and an amine functionality in one molecule [18]. Oligo- and polymerization of these can potentially lead to new polyamides, or to non-natural peptide mimetics that integrate some of the chiral information of carbohydrates [19]. Surface attachment of such structures can result into new grafts, imitating those of cell wall integrated proteins or oligosaccharides. An unproven advantage of ASA *C*-glycosides could be the suppression, control, or study of glucosidase cleavages [20].

As a proof of concept this work investigates the modification of thin, nanometric chitosan layers (Fig. 1), where chitosan has the advantage of abundance and biocompatibility over synthetic polyamine surfaces [21].

These layers are used to covalently attach a fluorescently labelled, previously synthesized *C*-glycosidic furanose amino sugar acid, and fluorescently labelled aminohexanoic acid (AHX) derivatives. In this way novel, well defined functionalized polysaccharide interfaces are created, that are characterized in detail with respect to the bound molecules and their morphology using fluorescence scanning, X-ray photoelectron spectroscopy (XPS), time-of-flight secondary ion mass spectrometry (ToF–SIMS), and atomic force microscopy (AFM) measurements. This work serves as a basis for the functionalization of chitosan/chitin layers with a furanose type *C*-glycoside ASA, and with a lysine analogue type AHX, with the aim of creating an unambiguous, semi-synthetic model for further biofunctionalization. It reports novel results on the conditions and analytics necessary to

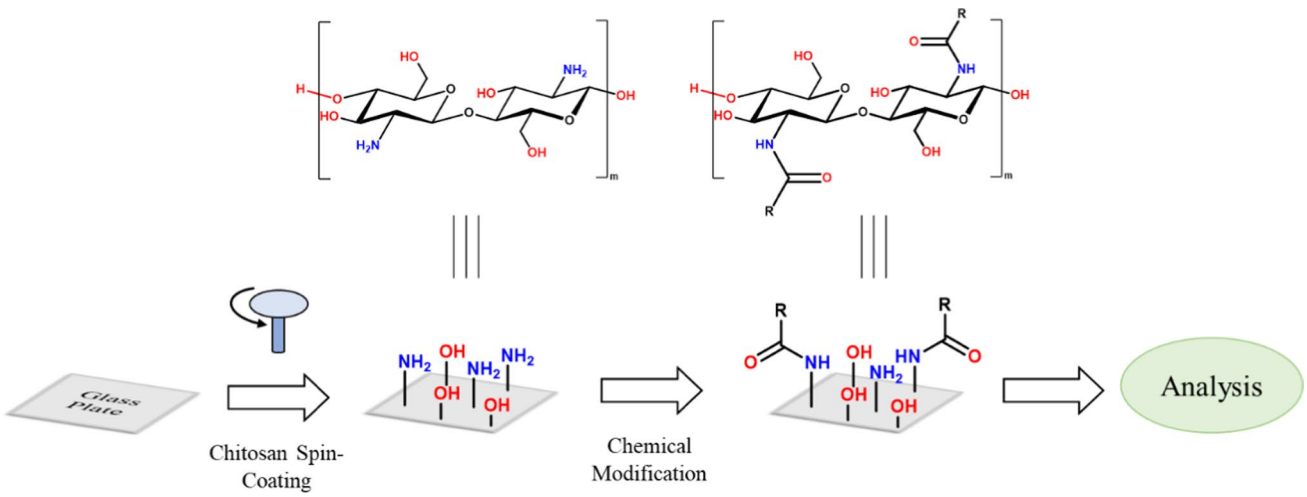

Fig. 1 Targeted modification pathway of chitosan thin films with different fluorescent small molecules (depicted as R) as amides

attach saccharide analogues to polyamine bearing surfaces. This can be extended to the binding of glycoside hydrolase inhibitors in future works.

Results and discussion

Fluorescence measurements

As reported previously, spin coating of chitosan (CHI) resulted in stable reproducible thin films with a thickness of 32 ± 3 nm [22]. Fluorescence measurements indicated the presence of the desired fluorescent-labelled molecules **1**—**3** (Fig. 2) on chitosan spin-coated glass slides after the amide coupling with 1-ethyl-3-(3-dimethylaminopropyl)carbodiimide (EDC). Fluorenylmethyloxycarbonyl (Fmoc)-modified plates (CHI_FmocAHX **1**) were measured at the literature known excitation of 270 nm and emission of 315 nm [23], whereas for the dansyl (Dan) group (CHI_DanAHX **2**, CHI_DanSugar **3**) the excitation was set to 350 nm and the emission measured at 520 nm [24]. Figure 3 shows surface scans with a 3D-printed slide holder in a microplate reader of the glass slides for the dansyl and Fmoc moieties **1**, **2**, and **3**, respectively. The fluorescence intensities are evenly distributed over the surface, indicating a uniform modification. Only in the case of CHI_FmocAHX, a small gradient is visible, which is not expected to have implications for further use of the modified slides, as it does not imply a difference in surface concentration of the attached molecules. A slight deviation in film thickness or an uneven placement in the slide holder can also lead to fluctuations in the fluorescence signal, as the distance from the surface to the detector changes. In general, the modification was reproducible and only in a few cases, imperfections in the fluorescence scans could be seen.

The measured intensity of the dansylated carbohydrate **3** is lower than the intensity of the dansylated AHX derivative **2**, which could mean a lower degree of substitution, believed to be a result of steric hindrance.

In contrast to the slides in Fig. 3, where the covalent modification was enabled by a carbodiimide coupling, the control slides, where no EDC was added to activate the carboxylic acid, showed no fluorescence (Fig. 4). This indicates the desired covalent attachment of the target molecules to the surfaces instead of, e.g. ionic interactions, as the non-covalently bound molecules could be removed in the washing step.

In general, the use of the 3D-printed slide holder and a microplate reader enables a fast and easy qualitative method for surface fluorescence scans. While some comparisons between the fluorescence intensity between different glass plates measured at the same time can be made, a quantification was not attempted.

Topography

AFM measurements (Fig. 5) show uniform surfaces with no, to only minor inhomogeneities and without larger film defects or macropores. The root mean square (RMS) roughness of the films is between 2.34 and 5.21 nm but no clear correlation between the surface treatments and the changes in roughness can be established. It however seems obvious, that the chemical treatments and washing steps do not visibly damage the thin films.

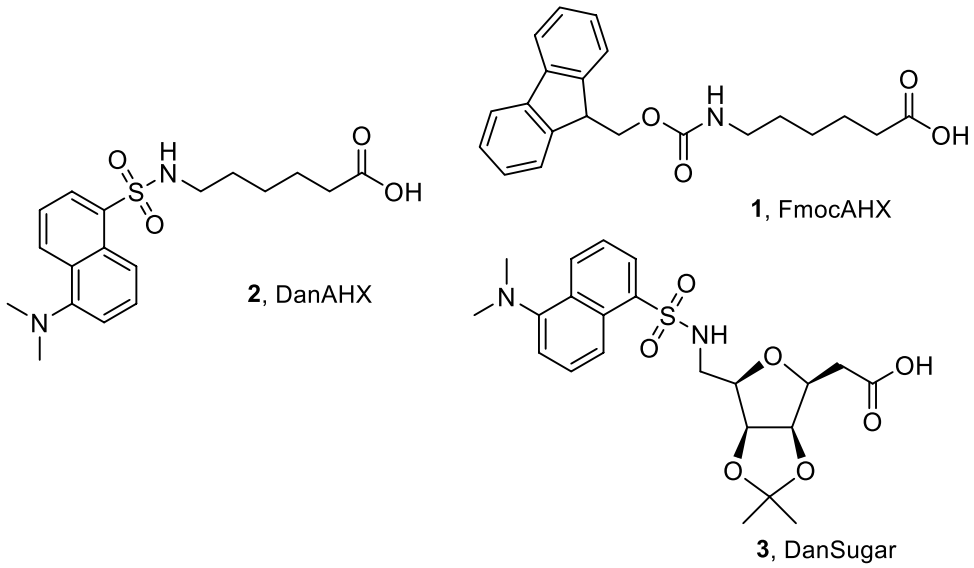

Fig. 2 Target molecules **1**–**3** for the modification of spin-coated chitosan thin films

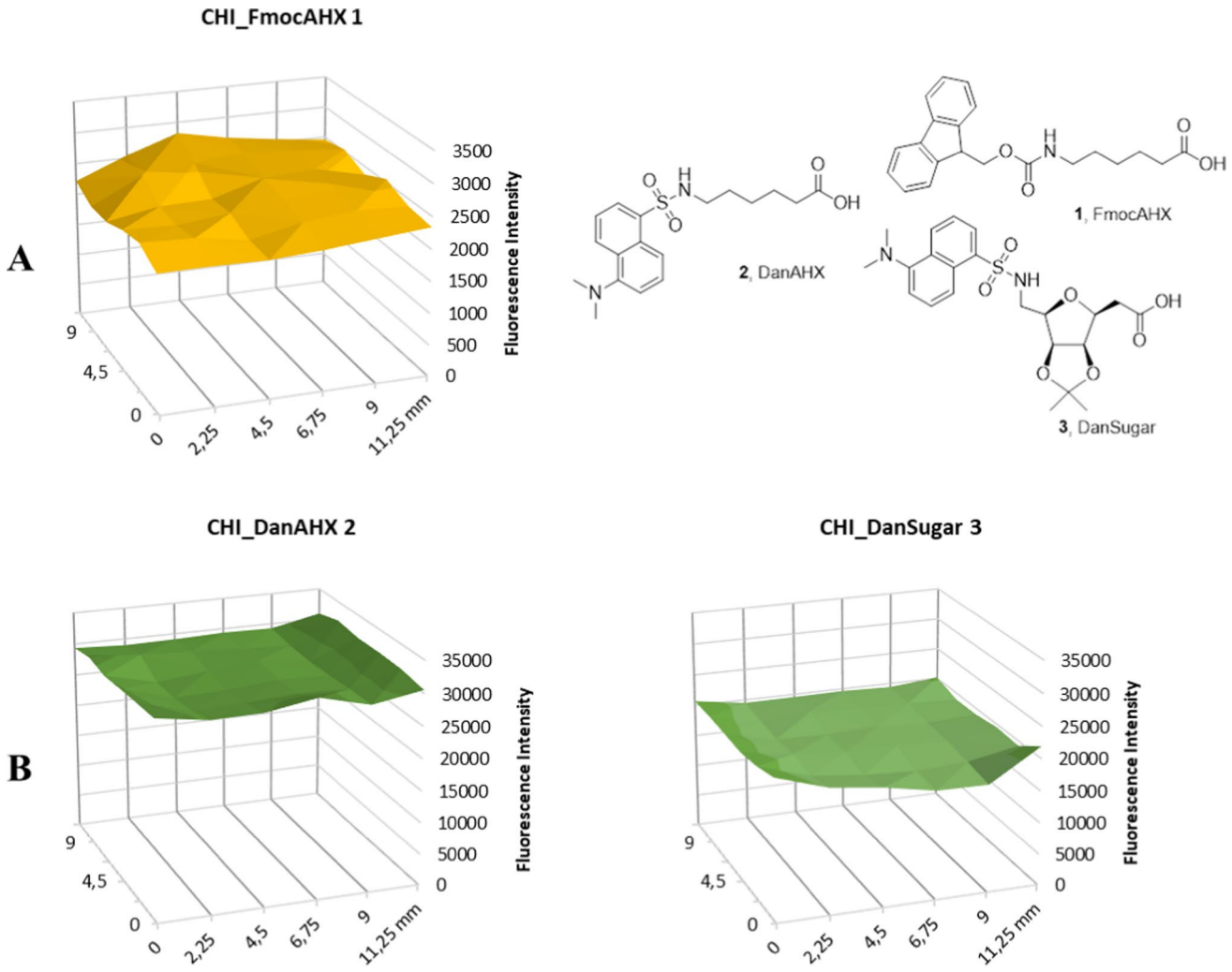

Fig. 3 Fluorescence intensity scans of the modified chitosan surfaces. The first row (**A**) shows the Fmoc scans (excitation 270 nm, emission 315 nm). The second row (**B**) shows the dansyl scans (excitation 350 nm, emission 520 nm)

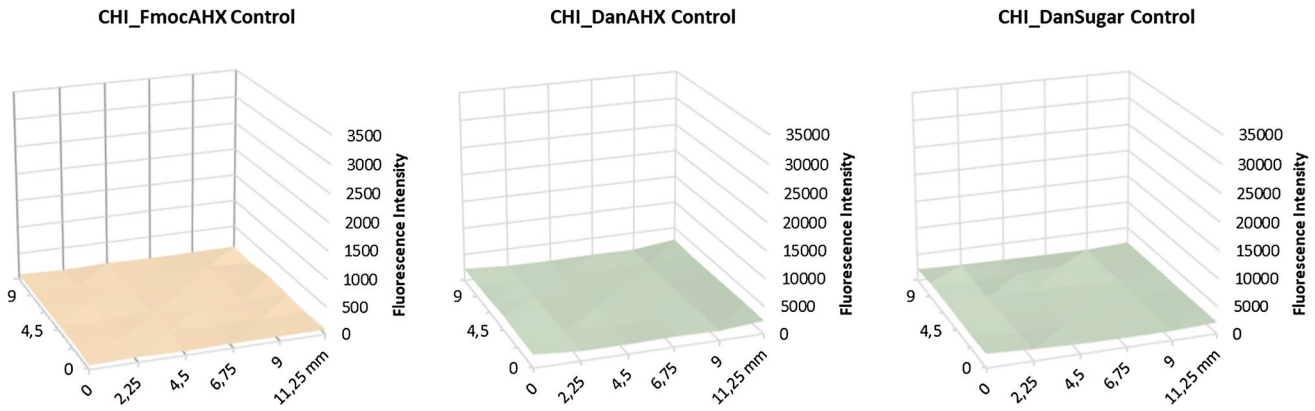

Fig. 4 Fluorescence intensity scans of the control slides. Fmoc scan taken at an excitation of 270 nm and an emission of 315 nm. Dansyl scans taken at an excitation of 350 nm and an of emission 520 nm

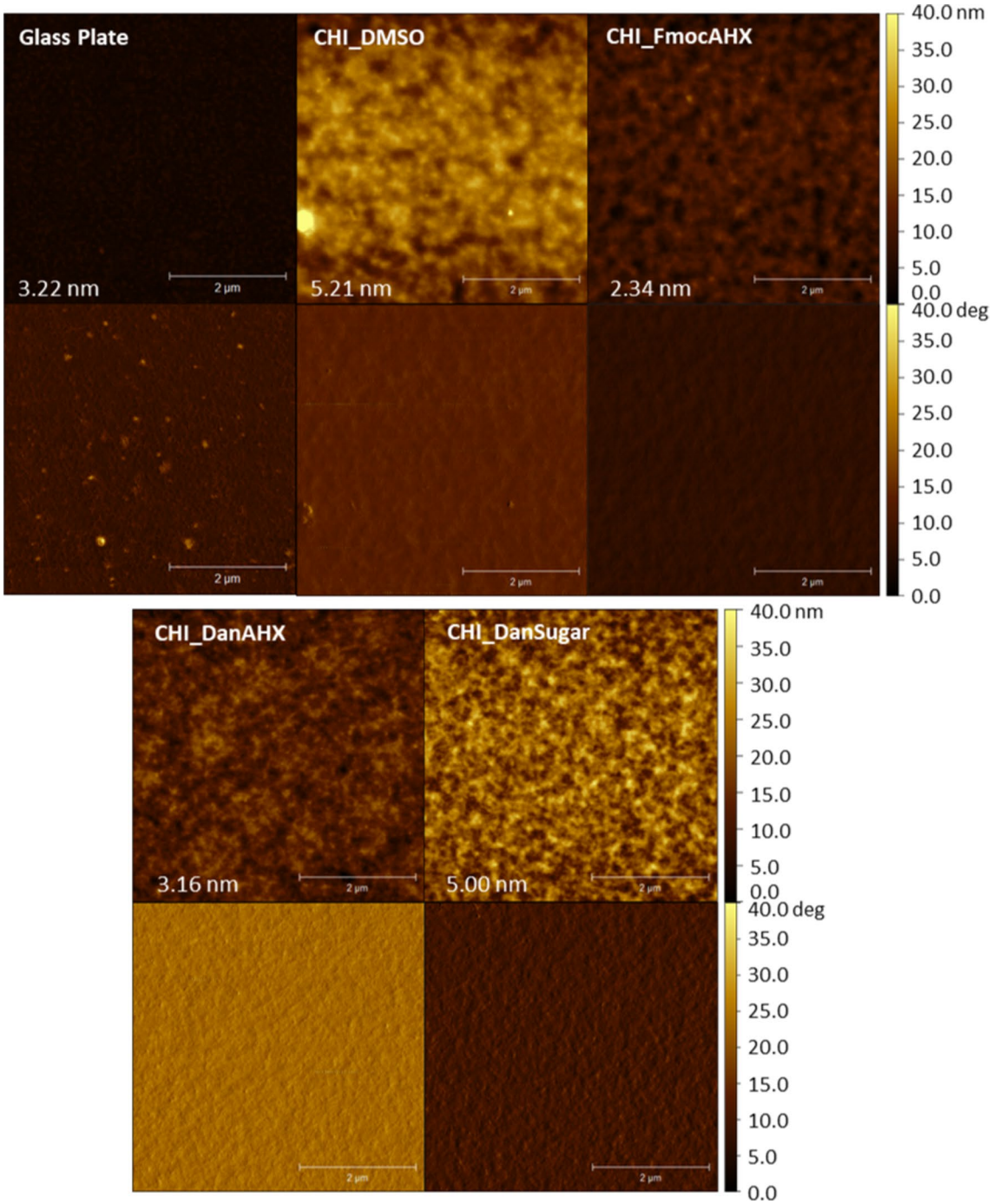

Fig. 5 AFM topography and phase images (5 µm × 5 µm) of the modified chitosan surfaces. RMS roughness values are shown

Surface composition

To further confirm the presence of the target molecules on the surfaces and verify the uniformity, ToF–SIMS imaging was performed. All samples showed an even distribution of typical chitosan derived fragments and only small inhomogeneities, with CHI_DMSO shown in Fig. 6A as an example. For the target molecules, specific fragments characterizing organic molecules were chosen and are visualised in Fig. 6B, C, and D. In accordance with the fluorescence data, the target molecules are evenly distributed on the surfaces. Only in the case of CHI_FmocAHX (Fig. 6B), a small gradient is visible, which is also seen in the fluorescence data and can originate from the spin coating process.

XPS measurements gave further insight into the atomic composition of the surfaces. Figure 7 shows C 1 s and Fig. 8

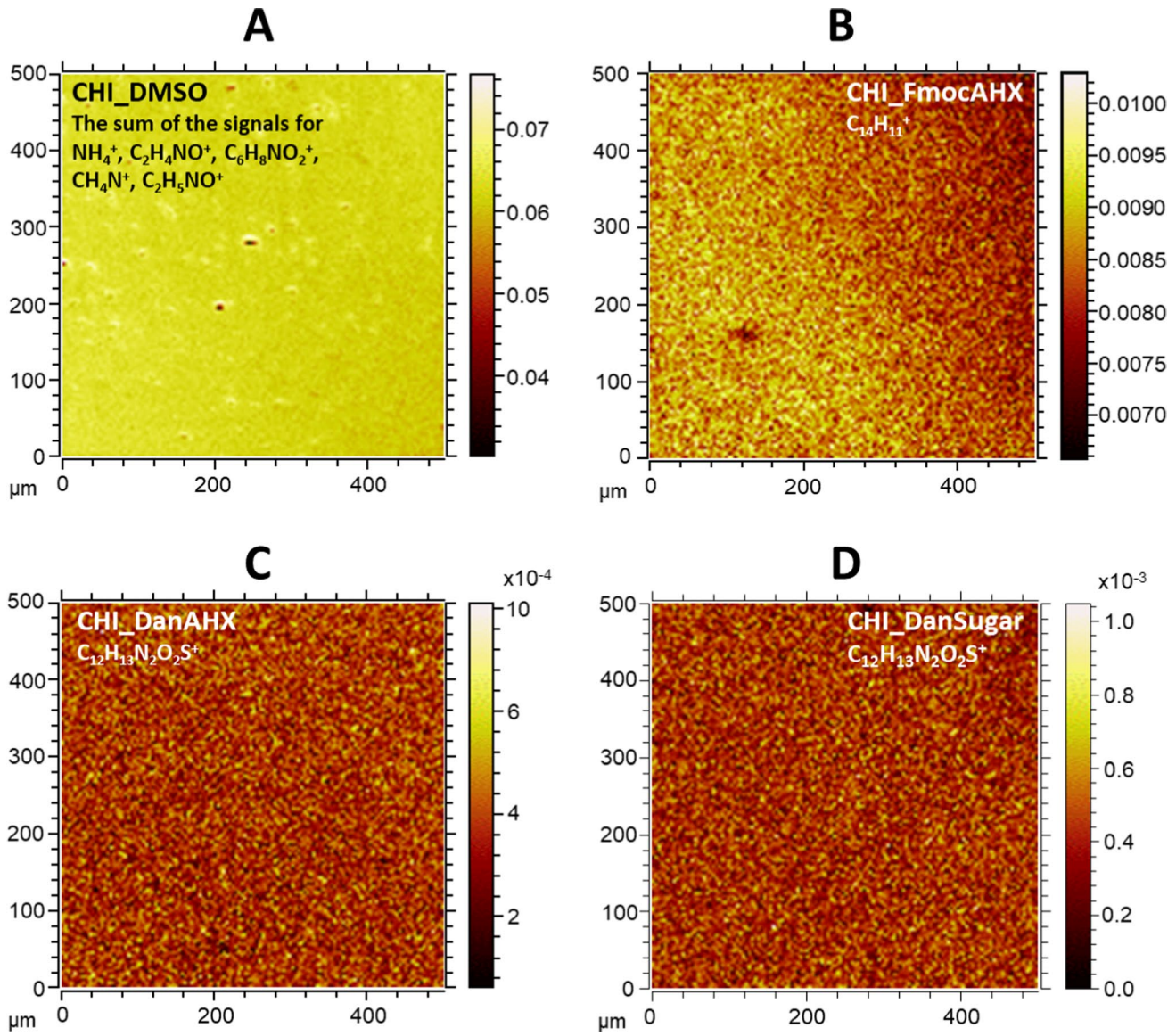

Fig. 6 ToF–SIMS imaging (500 μm × 500 μm) of the modified chitosan surfaces. **A** CHI_DMSO (The sum of the signals for NH_4^+, $C_2H_4NO^+$, $C_6H_8NO_2^+$, CH_4N^+, and $C_2H_5NO^+$), **B** CHI_FmocAHX ($C_{14}H_{11}^+$), **C** CHI_DanAHX ($C_{12}H_{13}N_2O_2S^+$), **D** CHI_DanSugar ($C_{12}H_{13}N_2O_2S^+$). Intensities were normalised to the total ion signal

N 1 s measured and fitted XPS spectra. The typical XPS measurement errors were never higher than 0.7% of the measured atomic concentration (Tables S1–S4).

The surface atomic concentration of C atoms in O=C–O/O=C–N is similar (between 12.7 and 17.6%) for all samples. The used commercial chitosan has a deacetylation grade of 75–85%, meaning that the O=C–O/O=C–N for all samples can be attributed to the 15–25% acetyl groups on the chitosan or to the bound substituents.

The surface atomic concentration of C–O (peak located at 286.4 eV) can mainly be attributed to the hydroxyl functions of the chitosan thin films. After the modification, the C–C/C–H surface atomic concentration (peak located at 284.8 eV) is expected to increase for the samples CHI_FmocAHX, CHI_DanAHX, and CHI_DanSugar, when compared to CHI_DMSO (Fig. 5). In the cases of CHI_DanAHX and CHI_DanSugar, the C–C/C–H surface atomic concentration has increased compared to the CHI_DMSO sample. However, in the case of CHI_FmocAHX, the surface atomic concentration of C–C/C–H has decreased. The differences in the fractions could therefore also be explained by contamination from the air or from the solvents during the handling and transport of the samples contributing to the C–C/C–H peak for the unmodified sample. In general, the measured C 1 s spectra are similar to known XPS spectra of pure chitosan [25].

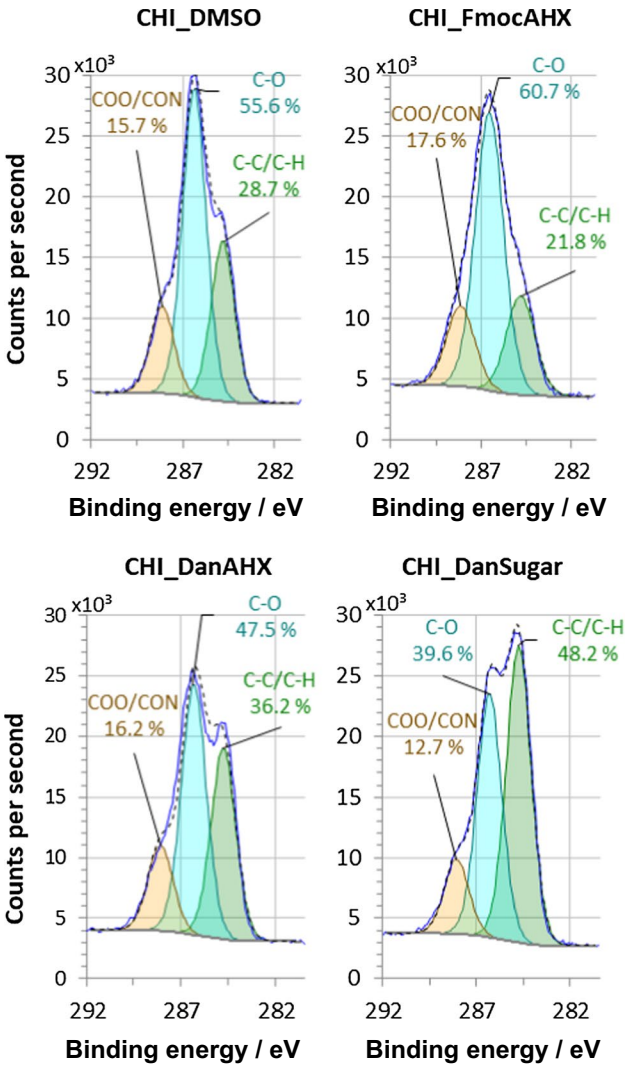

Fig. 7 XPS measurements of the modified chitosan surfaces. C 1 s fitted spectra for CHI_DMSO, CHI_FmocAHX, CHI_DanAHX, CHI_DanSugar

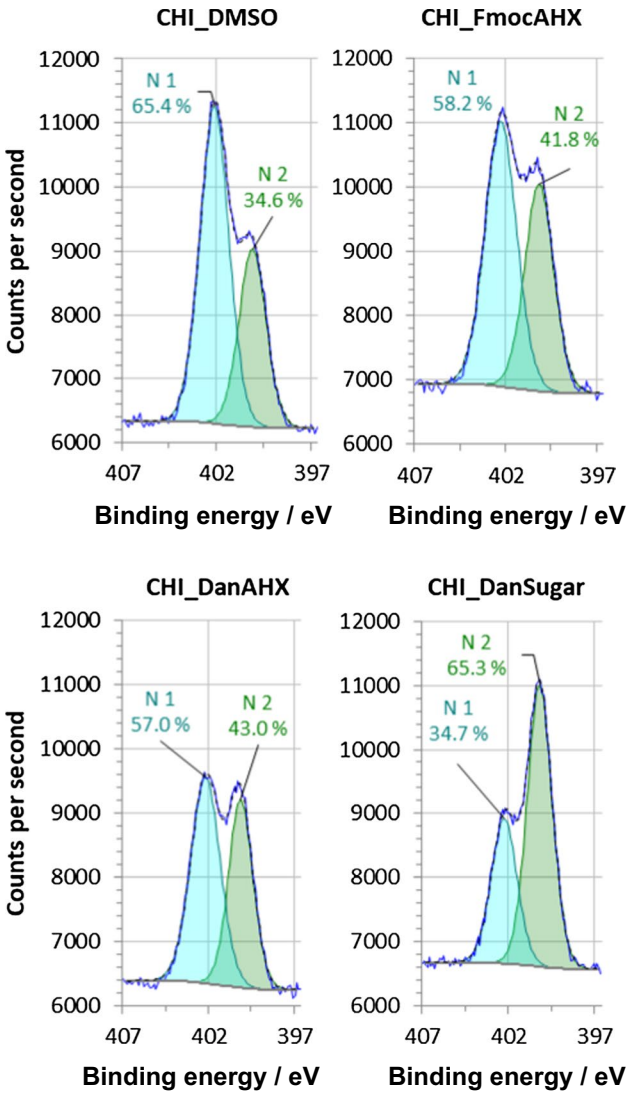

Fig. 8 XPS measurements of the modified chitosan surfaces. N 1 s fitted spectra for CHI_DMSO, CHI_FmocAHX, CHI_DanAHX, CHI_DanSugar

Figure 8 shows XPS N 1 s spectra with two deconvoluted peaks. The peak (designated N 1) located at 401.9 eV can be assigned to protonated NH_3^+ groups, the second one (designated N 2) located at 399.8 eV is ascribed to non-protonated NH_2 groups of the chitosan. An increase in the surface atomic concentration of N in NH_2/NH compared to NH_3^+ is expected after the modification, as the desired formation of the amide bonds or neutralization would decrease the fraction of protonated NH_3^+ groups on the chitosan [22]. In the cases of CHI_FmocAHX and CHI_DanAHX, the surface atomic concentration of N in NH_2/NH is slightly increased compared to CHI_DMSO, while in the case of CHI_DanSugar the surface atomic concentration of N in NH_2/NH is higher than in all other samples studied. These results support the successful binding of the target molecules to the chitosan thin films.

Conclusion

The chemical modification of chitosan thin films with fluorescent aminohexanoic acids and a synthetic sugar amino acid could be demonstrated. The chitosan layers are comparable to synthetic polyamine surfaces for the immobilization of similar classes of molecules [7, 21] but have the advantage of being non-toxic, renewable, stereo-chemically more complex, and comprised of saccharide units. This could allow regioselective modification or specific enzymatic degradation in the future. Chitosan has also the advantage of a pH-value-dependent solubility, which can be used to influence the stability of the thin layers [22]. Fluorescence measurements of the thin film functionalized glass slides enabled a fast and straightforward way to confirm the stable

covalent binding, while ToF–SIMS and XPS measurements gave further qualitative insight into the surface composition.

An open challenge is to quantify the degree of substitution and to confirm the type of bond formed between the chitosan and the small molecules (Fig. 9). It is hypothesized that the carbodiimide coupling in DMSO preferentially forms amide bonds with the carboxylic acids of the small molecules and the amine in the C2 position of the polymer. The formation of esters with the hydroxyl groups without the addition of a catalyst such as DMAP is less likely [26]. However, while the amide bond is chemically more resistant, the ester bonds should also be stable under the physiological conditions where future enzyme or cell tests will be conducted.

The FMOC protecting group opens the possibility to build larger (pseudo-)peptides on these surfaces as well as the binding of enzyme inhibitors, such as iminosugars for glycoside hydrolases [27]. Subsequently, the interaction with such enzymes using QCM-D or SPR biosensors, or in a further step living cells, can be studied (Fig. 10).

Experimental

Chitosan thin film preparation

Chitosan thin films were prepared as previously described [22]. Summarised, 2.5 cm × 2.5 cm glass slides were cut from regular microscope slides. The glass slides were cleaned using "piranha" solution (H_2SO_4/30% H_2O_2 3/1 *v/v, caution, strongly exothermic and corrosive*), spin-coated (Table 1) with 500 mm^3 of a 1 wt.% chitosan solution (Sigma–Aldrich 448,869, 75–85% deacetylation, low molecular weight). The chitosan solution is prepared by dissolving

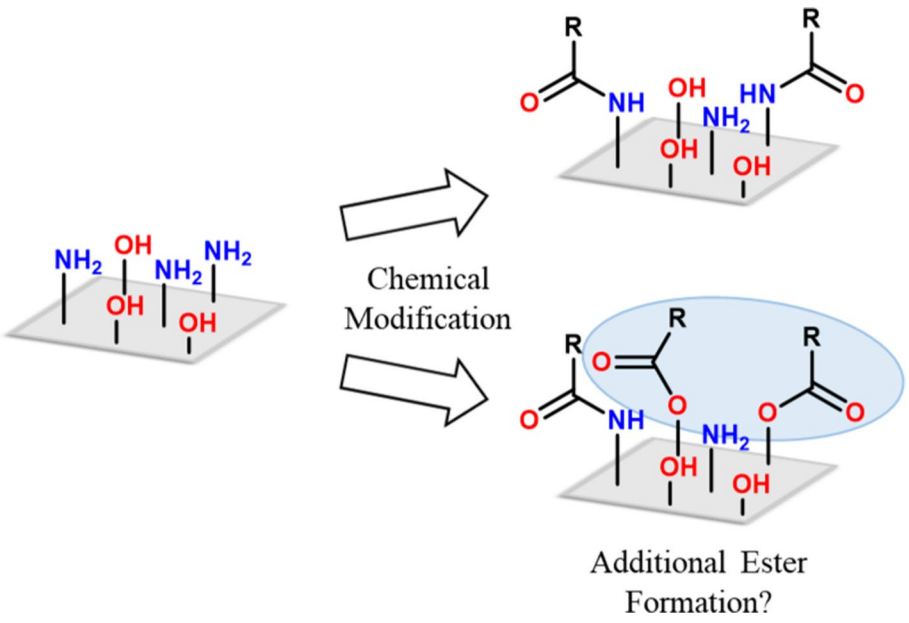

Fig. 9 An open question is the type of bond formed on the surface. While the more stable amide bond with the amino groups of the chitosan is preferred, also ester formation with free hydroxyl groups of the polysaccharide is theoretically possible

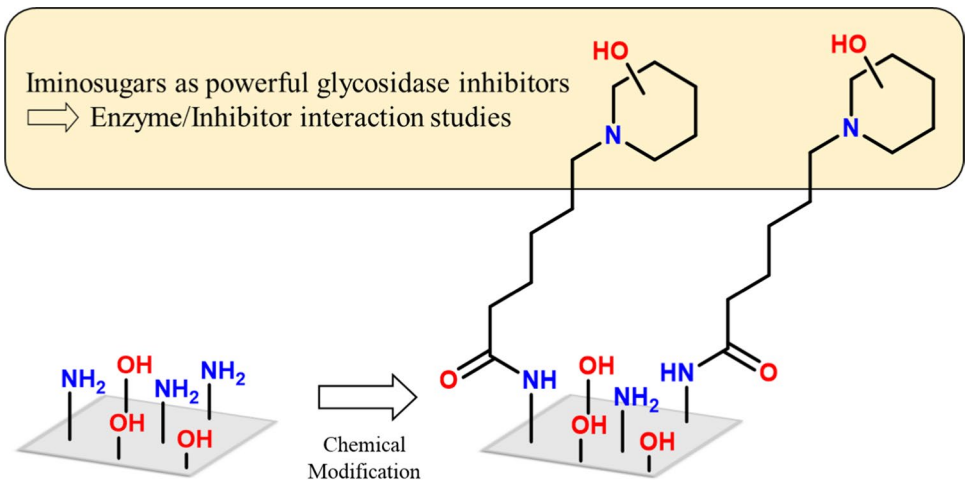

Fig. 10 In future work, chitosan thin films will be modified with glycosidase inhibitors, like imino sugars [27], to enable the study of enzyme/inhibitor interactions with, e.g. QCM-D measurements

Table 1 Spin-coating program for the preparation of chitosan thin films [22]

Step	Speed/rpm	Duration/s
Surface wetting	10	10
Solution spreading	5000	30
Drying	2000	30

chitosan in a minimal amount of 0.1 M HCl at pH 2, stirring for 1 h, then adjusting the pH to 5 with 0.1 M NaOH solution, addition of water to the desired chitosan concentration and filtering through a PTFE syringe filter (pore size 1 µm) three times. After spin-coating, the surfaces are neutralized in 0.5 M aqueous NaOH solution, to deprotonate the amines and make the surface water insoluble. The chitosan-modified glass slides were stored in a vacuum desiccator over calcium chloride until further use.

Synthesis

Three different fluorescent labelled molecules were used for the chemical modification of the chitosan thin films shown in Fig. 1. 6-(Fmoc-amino)hexanoic acid (FmocAHX, **1**), which is commercially available, was chosen as it can be used as a spacer for subsequent modification after removal of the Fmoc protecting group. To use a better fluorophore for fluorescence measurements, dansylated 6-aminohexanoic acid (DanAHX, **2**) was prepared as described in the literature [28]. The third target molecule, a dansylated *C*-glycosidic mannose derivative **3**, was used to explore the possibility of more complex compounds on the surface. The synthesis of compound **3** is described in the Supporting Info.

Chitosan modification

For each 2.5 cm × 2.5 cm glass plate, 60 µmol of the target molecule was dissolved in 5 mm^3 DMSO and 60 µmol of EDC hydrochloride was added. The reaction mixture was stirred at r.t. until all solids were dissolved, which typically took 5 min. The solution was then added to a crystallizing dish and the spin-coated glass plate was immersed overnight. For the blank slide (CHI_DMSO), a spin-coated glass slide was immersed in DMSO overnight. Additionally, to verify if the target molecules are covalently bound and not physically adsorbed to the surfaces, glass slides were immersed in solutions of the target molecules in DMSO without EDC hydrochloride for the same amount of time.

Each glass slide was subsequently immersed and washed with DMSO, water, acetone, and dichloromethane. They were dried using nitrogen gas and stored in a vacuum desiccator over calcium chloride until further use.

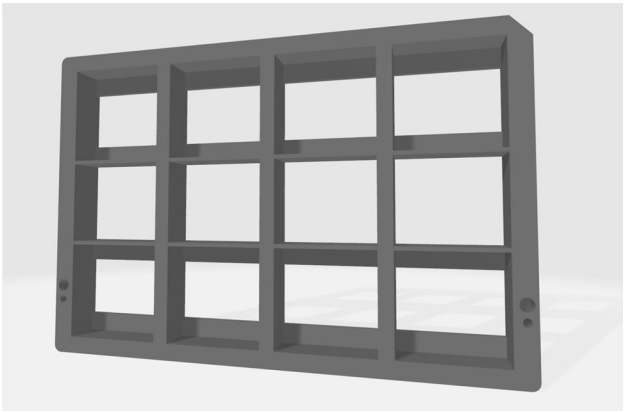

Fig. 11 3D-printed slide holder for fluorescence measurements. 3D model modified from [29]

Fluorescence spectroscopy

Fluorescence intensities were recorded on a Tecan Spark Microplate Reader using a custom modified, 3D-printed slide holder (Fig. 11) [29]. The surfaces were scanned with the grid of a 1536 well plate, resulting in a measured area of about 11 mm × 11 mm per glass slide.

AFM measurements

Atomic force microscopy images were recorded on a Tosca 400, Anton Paar. The images were scanned at room temperature in tapping mode with a silicon SPM-Sensor (Arrow-NCR-50, Nanoworld, Switzerland, resonance frequency 285 kHz, force constant 42 N/m). Image sizes of 10 µm × 10 µm, 5 µm × 5 µm, and 1 µm × 1 µm were scanned at a speed of 0.9 lines per second. Image processing was done using Gwyddion [30].

XPS measurements

XPS measurements were performed using Supra plus device (Kratos, Manchester, UK) equipped with an Al K_α excitation source. Measurements were performed on a 300 by 700 µm spot size at 20 eV pass energy and 90° take-off angle. During the spectra acquisition, the charge neutralizer was on. XPS measurements and data processing were performed with ESCApe 1.5 software (Kratos). Shirley background subtraction was employed. The binding energy scale was corrected using the C–C/C-H peak at 284.8 eV in the C 1 s spectra. The base pressure in the main analysis chamber during the measurements was in the range of 10^{-10} torr.

ToF–SIMS measurements

ToF–SIMS measurements were performed with M6 device (IONTOF, Münster, Germany) controller by the SurfaceLab 7.3 software (IONTOF). The base pressure in the main analysis chamber during the measurements was in the range of 10^{-11} torr. To compensate for the charge created during the measurements, the flood gun was on, and additional flooding with argon gas (5×10^{-7} mbar) was applied. 2D-imaging was performed with the instrumental settings in that the lateral resolution was about 1 µm, and the mass resolution was around 10 000. The mass spectra were calibrated with the peaks at known mass-to-charge ratio (*m/z*).

Supplementary Information The online version contains supplementary material available at https://doi.org/10.1007/s00706-024-03227-y.

Acknowledgements Support from NAWI Graz is gratefully acknowledged. The authors would like to acknowledge use of the Somapp Lab, a core facility supported by the Austrian Federal Ministry of Education, Science and Research, the Graz University of Technology, the University of Graz and Anton Paar GmbH. The financial support received from the Slovenian Research Agency (grant No. P2-0118) is hereby gratefully acknowledged. The project is co-financed by the Republic of Slovenia, the Ministry of Education, Science and Sport, and the European Union through the European Regional Development Fund.

Funding Open access funding provided by Graz University of Technology.

Data availability Not applicable.

References

1. Vollmer W, Blanot D, De Pedro MA (2008) FEMS Microbiol Rev 32:149
2. Gow NAR, Latge JP, Munro CA (2017). Microbiol Spectrum. https://doi.org/10.1128/microbiolspec.FUNK-0035-2016
3. Moore KH, Murphy HA, George EM (2021) Am J Physiol: Regul Integr Comp Physiol 320:508
4. Mende M, Tsouka A, Heidepriem J, Paris G, Mattes DS, Eickelmann S, Bordoni V, Wawrzinek R, Fuchsberger FF, Seeberger PH, Rademacher C, Delbianco M, Mallagaray A, Loeffler FF (2020) Chem Eur J 26:9954
5. Orelma H, Teerinen T, Johansson LS, Holappa S, Laine J (2012) Biomacromol 13:1051
6. Kargl R, Mohan T, Köstler S, Spirk S, Doliška A, Stana-Kleinschek K, Ribitsch V (2012) Adv Funct Mater 23:308
7. Steiner AJ, Stütz AE, Wrodnigg TM, Tarling CA, Withers SG, Hermetter A, Schmidinger H (2008) Bioorg Med Chem Lett 18:1922
8. Joseph AA, Pardo-Vargas A, Seeberger PH (2020) J Am Chem Soc 142:8561
9. Mohan T, Kargl R, Tradt K, Kulterer M, Bračić M, Hribernik S, Stana-Kleinschek K, Ribitsch V (2015) Carbohydr Polym 116:149
10. Fält S, Wågberg L, Vesterlind EL (2003) Langmuir 19:7895
11. Kargl R, Vorraber V, Ribitsch V, Köstler S, Stana-Kleinschek K, Mohan T (2015) Biosens Bioelectron 68:437
12. Mohan T, Nagaraj C, Nagy BM, Bračič M, Maver U, Olschewski A, Stana-Kleinschek K, Kargl R (2019) Biomacromol 20:2327
13. Frank R (2002) J Immunol Methods 267:13
14. Kumari S, Tiyyagura HR, Pottathara YB, Sadasivuni KK, Ponnamma D, Douglas TEL, Skirtach AG, Mohan MK (2021) Carbohydr Polym 255:117487
15. Bui CV, Rosenau T, Hettegger H (2023) Cellulose 30:2337
16. Buckley LF, Reardon DP, Camp PC, Weinhouse GL, Silver DA, Couper GS, Connors JM (2016) Heart Lung 45:232
17. Yazawa K, Numata K (2016) Polymers 8:194
18. Chakraborty TK, Srinivasu P, Tapadar S, Mohan BK (2005) Glycoconjugate J 22:83
19. Tian G-Z, Wang X-L, Hu J, Wang X-B, Guo X-Q, Yin J (2015) Chin Chem Lett 26:922
20. Mori T, Kumano T, He H, Watanabe S, Senda M, Moriya T, Adachi N, Hori S, Terashita Y, Kawasaki M, Hashimoto Y, Awakawa T, Senda T, Abe I, Kobayashi M (2021) Nat Commun 12:6294
21. Gupta A, Gupta GS (2022) J Nanopart Res 24:228
22. Katan T, Kargl R, Mohan T, Steindorfer T, Mozetič M, Kovač J, Stana Kleinschek K (2022) Biomacromol 23:731
23. Shangguan D, Zhao Y, Han H, Zhao R, Liu G (2001) Anal Chem 73:2054
24. Ren B, Gao F, Tong Z, Yan Y (1999) Chem Phys Lett 307:55
25. Maachou H, Genet MJ, Aliouche D, Dupont-Gillain CC, Rouxhet PG (2013) Surf Interface Anal 45:1088
26. Neises B, Steglich W (1978) Angew Chem Int Ed 17:522
27. Stütz AE, Wrodnigg TM (2011) Adv Carbohydr Chem Biochem 66:187
28. Hermetter A, Scholze H, Stütz AE, Withers SG, Wrodnigg TM (2001) Bioorg Med Chem Lett 11:1339
29. https://3d.nih.gov/entries/3dpx-012891 (Last visited: 07.05.2024), Damon Poburko (dpoburko@sfu.ca, http://www.sfu.ca/mcpg/Poburko.html).
30. Nečas D, Klapetek P (2012) Cent Eur J Phys 10:181

Authors and Affiliations

Tobias Dorn[1] · Matjaž Finšgar[2] · Karin Stana Kleinschek[1] · Tobias Steindorfer[1] · Martin Thonhofer[1] · Tanja M. Wrodnigg[1] · Rupert Kargl[1,3]

✉ Rupert Kargl
rupert.kargl@tugraz.at

[1] Institute for Chemistry and Technology of Biobased Systems, Graz University of Technology, Graz, Austria

[2] Faculty of Chemistry and Chemical Engineering, University of Maribor, Maribor, Slovenia

[3] Faculty of Mechanical Engineering, University of Maribor, Maribor, Slovenia